

The Combi-Targeting Concept: Synthesis of Stable Nitrosoureas Designed to Inhibit the Epidermal Growth Factor Receptor (EGFR)

Juozas Domarkas, Fabienne Dudouit, Christopher Williams, Qiu Qiyu, Ranjita Banerjee, Fouad Brahimi, and Bertrand Jacques Jean-Claude*

Cancer Drug Research Laboratory, Department of Medicine, Division of Medical Oncology, McGill University Health Center/Royal Victoria Hospital, Montreal, H3A1A1, Quebec, Canada

Received January 12, 2006

According to the “combi-targeting” concept, the EGFR tyrosine kinase (TK) inhibitory potency of compounds termed “combi-molecules” is critical for selective growth inhibition of tumor cells with disordered expression of EGFR or its closest family member *erbB2*. Here we report on the optimization of the EGFR TK inhibitory potency of the combi-molecules of the nitrosourea class by comparison with their aminoquinazoline and ureidoquinazoline precursors. This led to the discovery of a new structural parameter that influences their EGFR TK inhibitory potency, i.e., the torsion angle between the plane of the quinazoline ring and the ureido or the nitrosoureido moiety of the synthesized drugs. Compounds (3'-Cl and Br series) with small angles (0.5–3°) were generally stronger EGFR TK inhibitors than those with large angles (18–21°). This was further corroborated by ligand–receptor van der Waals interaction calculations that showed significant binding hindrance imposed by large torsion angles in the narrow ATP cleft of EGFR. Selective antiproliferative studies in a pair of mouse fibroblast NIH3T3 cells, one of which NIH3T3/*neu* being transfected with the *erbB2* oncogene, showed that IC_{50} values for inhibition of EGFR TK could be good predictors of their selective potency against the serum-stimulated growth of the *erbB2*-transfected cell line (Pearson $r = 0.8$). On the basis of stability ($t_{1/2}$), EGFR TK inhibitory potency (IC_{50}), and selective *erbB2* targeting, compound **23**, a stable nitrosourea, was considered to have the structural requirements for further development.

1. Introduction

The combi-targeting concept postulates that molecules termed “combi-molecules”, designed to block growth factor induced signaling on their own and to further degrade to a DNA-damaging species, should induce significant cell-killing in tumors resistant to classical alkylating agents of the same class. SMA41 and BJ2000 (Figure 1), the first molecular probes designed to verify the combi-targeting postulates, were shown to strongly block the epidermal growth factor receptor tyrosine kinase (EGFR TK) activity on their own in a short exposure enzyme assay.^{1,2} In addition, these molecules degraded in cell culture medium to generate a free aminoquinazoline, also capable of blocking EGFR TK on its own, and a DNA-alkylating methyl diazonium species. The formation of the latter has been proven by radiotracing.³ Thus, as outlined in Scheme 1, the combi-molecules TZ-I block EGFR TK on their own and degrade to another inhibitor I plus TZ, a DNA-damaging species. Both combi-molecules, SMA41 and BJ2000, were shown to possess significantly stronger potency than the clinical drug Temozolomide in cells coexpressing the DNA repair enzyme *O*⁶-alkylguanine transferase (AGT) and EGFR.⁴ SMA41 and BJ2000 being 1,2,3-triazenes, their half-lives were less than 1.5 h. Thus, to study the combi-targeting principles with more stable probes and to enhance their potency by releasing a bifunctional chloroethylating agent, we synthesized FD137 (**22**), a nitrosourea designed to release, like the triazenes, a free aminoquinazoline and a DNA-alkylating species.^{5,6} While FD137 was extremely stable ($t_{1/2} = 41$ h), its EGFR TK inhibitory activity ($IC_{50} = 1000$ nM) was more than 5-fold weaker than those of the triazenes. Here, we attempted to optimize the EGFR TK potency of this new class of molecules, termed combi-nitrosoureas, by

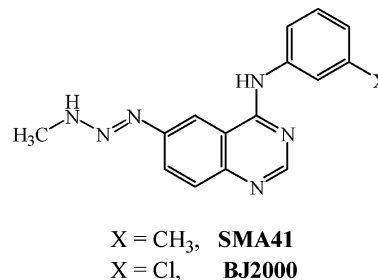
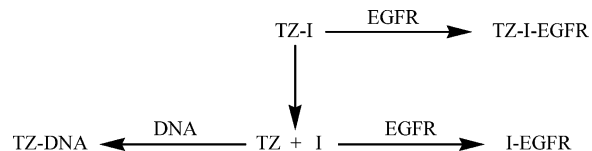


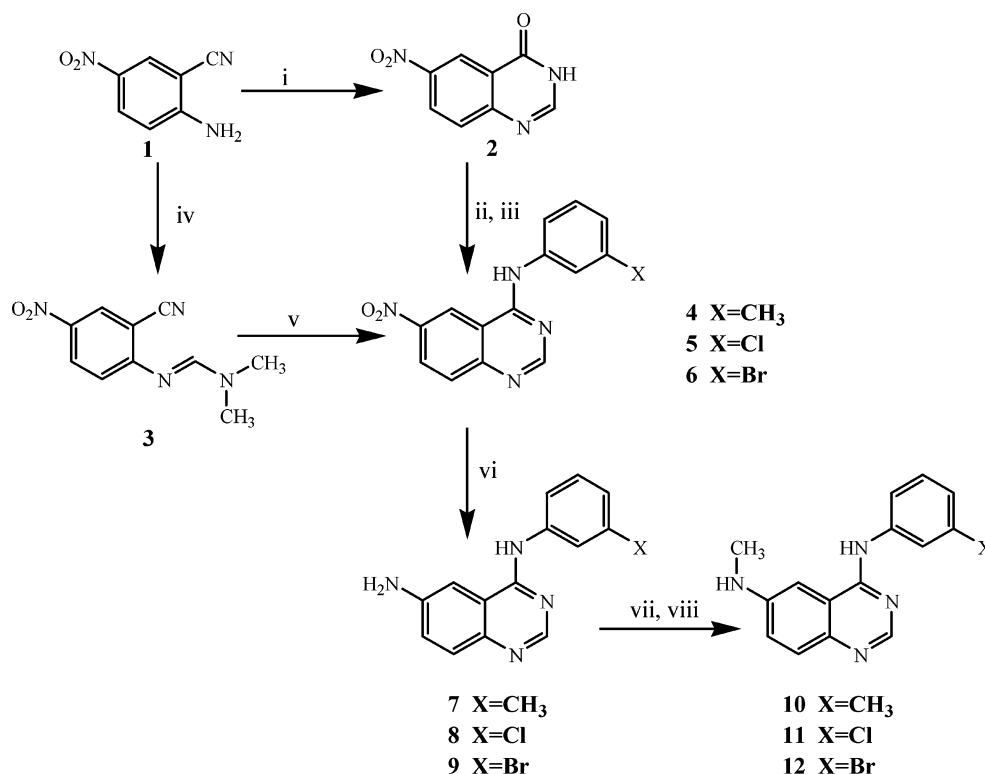
Figure 1. Structures of the first molecular probes SMA41 and BJ2000.

Scheme 1. Hydrolytic Pathway and Interactions Involved in the “Combi-Targeting” Strategy

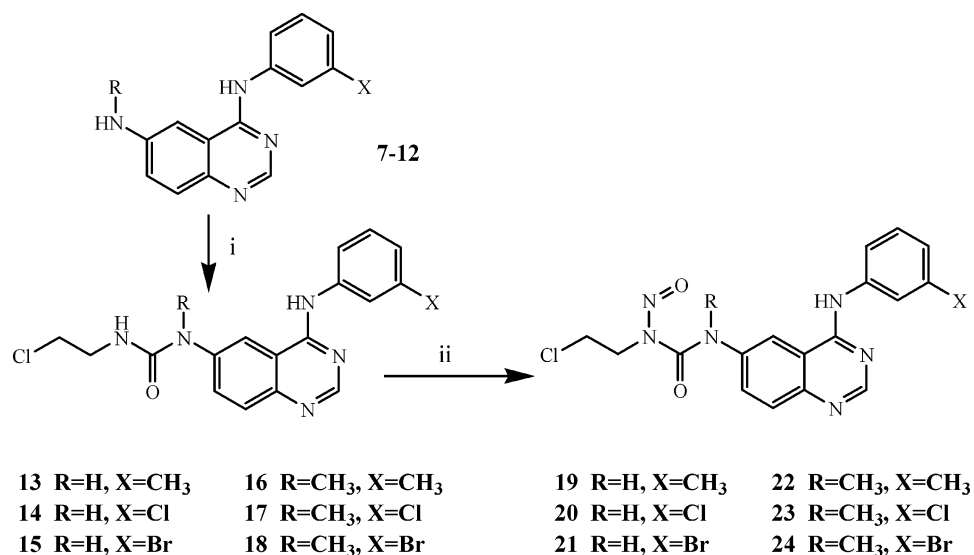


synthesizing a series of compounds with variable substituents at R on the ureido moiety and X on the aniline portion. Molecular modeling was used to rationalize the results and to develop a predictive equation for EGFR TK inhibitory potency of these agents based upon protein/ligand interaction energy (E_{int}), ligand bond stretch (E_{str}) and total strain energy (dE_{strain}). We also studied the correlation between the IC_{50} values for EGFR TK inhibition and the *erb* selectivity of these compounds in a pair of NIH3T3 wild-type and *erbB2*-transfected (NIH3T3/*neu*) cells. It should be remembered herein that the *erbB2* oncogene is overexpressed in a variety of solid tumors including breast, ovary, and prostate cancer cells and that this is associated with aggressive tumor progression and poor prognosis in the clinic.^{7–10}

* Corresponding author. Phone: (514) 934-1934 ext. 35841. Fax: (514) 843-1475. E-mail: bertrandj.jean-claude@mcgill.ca.

Scheme 2. Synthesis of Amines 7–12^a

^a (i) H₂SO₄/formic acid/reflux; (ii) PCl₅/160 °C; (iii) 3-methylaniline/2-propanol/60 °C; (iv) DMF–dimethyl acetal/reflux; (v) ArNH₂/AcOH/reflux; (vi) Pd(5%)/H₂(2 bar)/room temperature (X = CH₃) or Fe/AcOH/EtOH/H₂O/reflux (X = Cl, Br); (vii) EtOCOC/Cl/pyridine/0 °C; (viii) LiAlH₄/THF/reflux.

Scheme 3. Synthesis of Ureas 13–18 and Nitrosoureas 19–24^a

^a (i) 2-Chloroethylisocyanate/THF/0 °C; (ii) NOBF₄/AcOH/CH₃CN/0 °C.

2. Results and Discussion

2.1. Chemistry. The synthesis of the series proceeded as depicted in Schemes 2 and 3. 6-Aminoquinazolines 7–9 were prepared in three steps from nitroanthranilonitrile **1** as previously described.¹¹ Briefly, anthranilonitrile **1** was heated at reflux in formic acid containing concentrated H₂SO₄ to give 4-oxoquinazolinone **2**,¹¹ which was chlorinated with PCl₅ in fusion.¹² The resulting 4-chloroquinazolinone **4** which was catalytically reduced to amine **7**.¹³ Aminoquinazolines **8** and **9** were synthesized as per the procedure described by Tsou et al.¹⁴ Briefly, anthranilonitrile **1** was condensed with DMF–acetal

giving amidine **3**, which was cyclized in refluxing acetic acid in the presence of corresponding aniline to provide 6-nitroquinazolines **5** and **6**. Reduction of these nitro compounds with Fe gave the targeted amines **8** and **9** in good yield. 6-Aminoquinazolines 7–9 were converted to their N-methyl analogues **10–12** following a slightly modified procedure published by Bridges et al.¹⁵ First, amines 7–9 were treated with ethyl chloroformate, and then the resulting carbamates were reduced with LiAlH₄. The aminoquinazolines 7–12 thus generated were treated with 2-chloroethylisocyanate to provide ureas **13–18**, which were subsequently nitrosated with NOBF₄/AcOH to give nitrosoureas **19–24**. The latter compounds were purified by

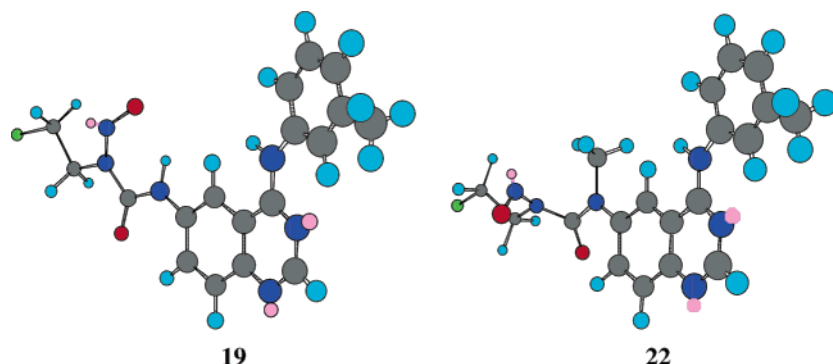


Figure 2. Three-dimensional views of energy-minimized structures of **19** (N3-H) and **22** (N3-methylated) nitrosoureas. Minimization was done and views generated by CS Chemdraw 3D Ultra 7.0 software, using the empirical MM2 method. See the Experimental Section for details.

Table 1. Half-lives ($t_{1/2}$) of the Combi-Nitrosoureas

compd	half-life ($t_{1/2}$)
19	30 min
20	15 min
21	26 min
22	41 h ^a
23	21 h 27 min
24	26 h

^a See ref 5.

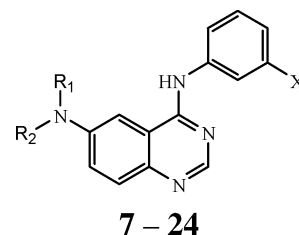
column chromatography on silica gel with a mixture of ethyl acetate/petroleum ether as eluent. The structures of various compounds were confirmed by ¹H, ¹³C NMR, and high-resolution mass spectrometry (HRMS).

2.2. Biology. 2.2.1. Stability of Combi-Nitrosoureas. As expected, the NH-unsubstituted nitrosoureas **19–21** were significantly less stable ($t_{1/2}$ = 15–30 min) than their N3-Me analogues **22–24**, the most stable compound remaining the 3'-methylanilinonitrosourea **22** ($t_{1/2}$ = 41 h) (Table 1). The half-lives of the 3'-halogenated compounds **23** and **24** were shorter ($t_{1/2}$ = 21–26 h), perhaps due to a more electron-withdrawing effect on the quinazoline ring that may translate into a relatively decreased electron density at the ureido N3 nitrogen.

2.2.2. EGFR Inhibitory Activity. Structure–activity relationships in the quinazolines already demonstrated that compounds containing a 3'-X = Br or Cl are consistently more potent than those with a methyl group.¹³ This trend was observed in all the series of compounds used herein whether they were aminoquinazolines, ureas or nitrosoureas. Many compounds with 3'-X = Me showed IC₅₀ in the 1 μM range, indicating little tolerance of bulkiness in the hydrophobic pocket of the ATP site of EGFR. In the amine series, the *N*-methylaminoquinazolines **10–12** were consistently more active than the primary amino ones **7–9**. This is in agreement with previous studies that showed significantly lower IC₅₀ values for *N*-monoalkylated aminoquinazolines when compared with those of the corresponding primary amines.¹⁵ Carbamylation of the primary 6-aminoquinazolines resulted in compounds with increased EGFR TK inhibitory potency. In contrast, carbamylation of *N*-methylaminoquinazolines consistently decreased EGFR TK inhibitory activities with a more pronounced effect in the 3'-methyl analogues. Finally, the nitrosation of N1 in the ureas, which slightly increases the bulkiness of the ureido moiety, did not show a consistent trend in the series.

We surmised that carbamylation of *N*-methylamino compounds led to a decrease in EGFR TK inhibitory activity due to the ability of the N3-Me group to impose a torsion angle between the plane of the aromatic quinazoline bicycle and that of the ureido function of the resulting molecules. This may lead

Table 2. Biological Activities of Aminoquinazolines, Ureidoquinazolines and Their Corresponding Combi-Nitrosoureas



no.	R ₁	R ₂	X	angle deg ^a	IC ₅₀ nM EGFR TK	IC ₅₀ , μM ^b	
						NIH3T3	NIH3T3/neu
7	H	H	Me		1000	44.2	6.39
8	H	H	Cl		200	97.0	3.29
9	H	H	Br		44	26.7	0.67
10	Me	H	Me		11	42.8	2.07
11	Me	H	Cl		4	49.8	0.89
12	Me	H	Br		5	17.6	0.17
13	H	CIEtNHCO	Me	0.69	676	31.0	2.10
14	H	CIEtNHCO	Cl	2.92	22	157.1	1.35
15	H	CIEtNHCO	Br	0.53	18	35.9	1.77
16	Me	CIEtNHCO	Me	19.44	1693	21.8	11.80
17	Me	CIEtNHCO	Cl	19.00	81	150.0	23.03
18	Me	CIEtNHCO	Br	19.12	156	60.5	11.08
19	H	CIEtN(NO)CO	Me	0.45	1061	78.5	12.18
20	H	CIEtN(NO)CO	Cl	0.56	67	157.0	5.40
21	H	CIEtN(NO)CO	Br	0.45	47	36.4	1.15
22	Me	CIEtN(NO)CO	Me	17.65	1139	16.5	6.88
23	Me	CIEtN(NO)CO	Cl	17.61	204	11.7	0.68
24	Me	CIEtN(NO)CO	Br	21.48	294	10.8	3.06

^a Torsion angles between ureido or nitrosoureido moieties and the quinazoline ring. ^b IC₅₀ values for inhibition of serum-stimulated growth after a 24 h of cell starvation.

to a less planar structure, a geometry that may hinder its binding in the ATP pocket of EGFR. Typical geometry-optimized structures of **19** and **22** are shown in Figure 2, and values for the calculated torsion angles between N3-H or N3-Me and the aromatic H7, representing the deviation of the ureido function from the quinazoline ring plane, are given in Table 2.

The nitrosourea **19** adopts an almost planar conformation with nitrosoureas function forming an internal hydrogen bond and a remarkably small torsion angle between N3-H and H7. The formation of intramolecular hydrogen bonds in nitrosoureas is now well documented.^{16–18} In contrast, in the N3-Me nitrosourea **22**, the oxygen of the nitroso group is pointed away from the methyl group and a torsion angle of 17.7° is observed between the latter group and H7, leaving a ureido group markedly deviated from the plane of the quinazoline ring. Similar results were obtained in the urea series, the trend being a small torsion angle (0.5–3°) for N3-H-containing ureas **13–15** and relatively larger angles (~19°) for N3-Me ureas **16–18**. As shown in the

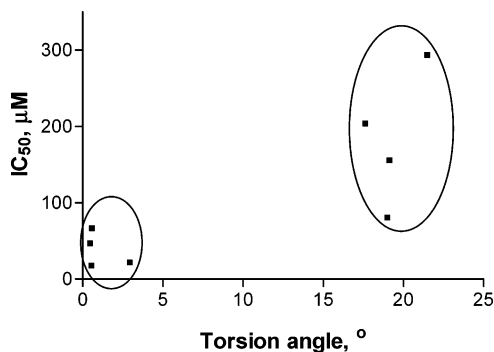


Figure 3. Relationship between the IC_{50} (EGFR TK) of the 3'-Cl and Br series and the torsion angles between the quinazoline bicycle and the ureido and nitrosoureido moieties.

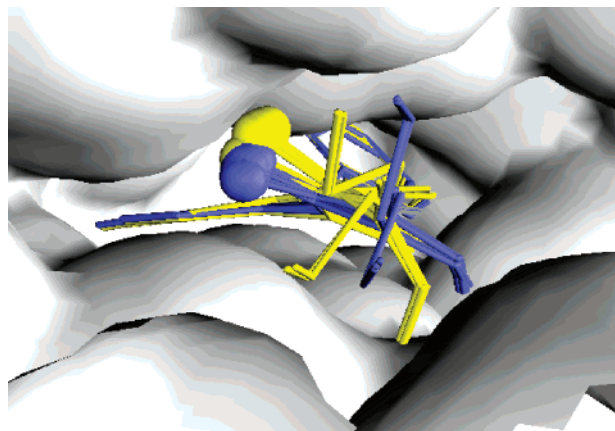


Figure 4. Compounds 7–24 overlaid in the EGFR TK ATP binding pocket. The carbonyl oxygen in each compound is shown as a ball. Structures with $R = CH_3$ are in yellow, while those of amines 7–12 and all others with $R = H$ are colored blue.

Figure 3, compounds with the large torsion angle were less active than those with small angles. As the range of IC_{50} values for the 3'-X = Me series was significantly different from those of the halogenated compounds, they were not plotted.

2.2.3. Conformation of Amines, Ureas and Nitrosoureas Docked into the EGFR ATP Binding Site. Analysis of X-ray structures of the TK domain of EGFR cocrystallized with 4-anilinoquinazoline showed that the pocket is quite narrow around the anilino and quinazoline ring systems but begins to open up a few angstroms away from the 6- and 7-positions of the quinazoline ring.¹⁹

A clear rationale for the geometry-dependent potency of the carbamoylated derivatives is depicted in Figure 4 wherein an overlay of all the refined compounds 7–24 in the EGFR TK ATP binding pocket is presented. The carbonyl oxygen in each compound is rendered as a ball for ease of visualization. The color scheme reflects the substitution at the R-position. Structures with $R = CH_3$ are in yellow, while structures of amines 7–12 and all other structures with $R = H$ are colored blue. Although all the structures may be docked and refined without unreasonable energy clashes, the view in Figure 4 clearly shows that the N3-methylated compounds have urea groups more out-of-plane with respect to the quinazoline ring than the nonmethylated ones. Furthermore, as the carbonyl group rotates out-of-plane with respect to the quinazoline ring, the carbonyl oxygen begins to collide with the van der Waals interaction surface, potentially increasing the van der Waals clash and decreasing binding affinity.

2.2.4. Defining a Structure–Activity Relationship (SAR) Based on Ligand–Receptor Interaction Energies. The ob-

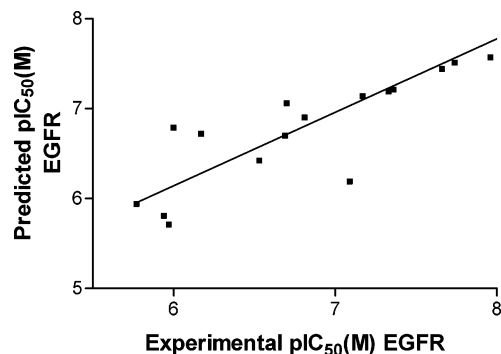


Figure 5. Predicted IC_{50} (EGFR TK) values vs the experimental IC_{50} (EGFR TK). (Pearson $r = 0.89$, P (one-tailed) < 0.0001).

servations that increasing the angle between the carbonyl and quinazoline planes could result in clashes with the receptor prompted further investigation of this effect as a possible explanation for the decreased activity of the N3-methylated compounds. A partial least-squares linear regression model of pIC_{50} (EGFR, M) was constructed in MOE using the MMFF94x energies as descriptors. The total protein/ligand interaction energy (E_{INT}) was used along with the ligand bond stretch (E_{STR}) and total (dE_{STRAIN}) strain energies to construct a QSAR model for compounds 7–24. The resulting QSAR equation (given below) has an $r^2 = 0.80$ and reflects the expected trend that increasing the strain energy values (E_{STR}) and (dE_{STRAIN}) will lower the pIC_{50} , while increasingly negative van der Waals interaction energies (E_{vdw}) will result in higher pIC_{50} .

$$pIC_{50}(\text{EGFR, M}) = 6.96 - 0.256E_{vdw} - 0.256dE_{strain} - 0.73468E_{str}$$

The plot of the predicted pIC_{50} versus the experimental values in Figure 5 shows that the QSAR model does reflect the activity with a general linear trend. The combination of this QSAR equation and observations made about the optimized ligands in the binding pocket suggest that binding of the N3-methylated ureas implies a greater deformation of the 6-position side chain than is required for the nonmethylated ureas. Although the methylated compounds can be made to fit into the binding pocket, this is only achieved at the cost of increasing the ligand strain energy.

2.3. Tumor Selectivity. Overexpression of EGFR and/or its closest related HER-2 receptor is correlated with unfavorable prognosis in patients with prostate and breast cancers. Overexpression of these receptors is also associated with reduced sensitivity to chemotherapeutic agents.^{20–23} To test the potency and selectivity of combi-molecules, we recently established a model in which the ability to block serum-stimulated proliferation of the NIH3T3 cell line is compared with that of NIH3T3 cells transfected with *HER-2* (NIH3T3/neu).^{24,25}

In the current study, a statistically significant correlation was observed between IC_{50} values for inhibition of EGFR TK and selective blockade $\log[IC_{50}(3T3/neu)/IC_{50}(3T3)]$ of serum-stimulated growth of *HER-2*-transfected cells by the various compounds (Figure 6). These results indicate that IC_{50} values for inhibition of EGFR TK represent good predictors for the *HER-2* selective potency of all the compounds analyzed herein, including the nitrosoureas, in this type of assay. This property may in principle be associated with the ability of the inhibitors to block serum-stimulated phosphorylation of the *HER-2* gene product and subsequent growth signaling. However, in non-growth-stimulated continuous exposure assays using the EGFR-expressing human prostate carcinoma cells LNCaP, we found

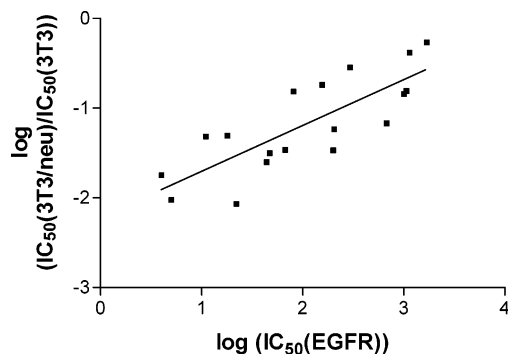


Figure 6. Correlation between IC_{50} (EGFR TK) and selective serum-stimulated growth inhibition of NIH3T3/neu-transfected cells (Pearson $r = 0.80$, P (one-tailed) < 0.0001).

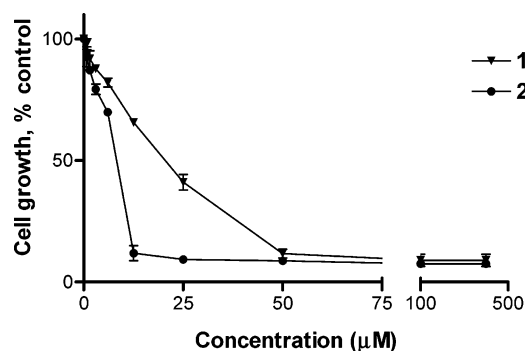
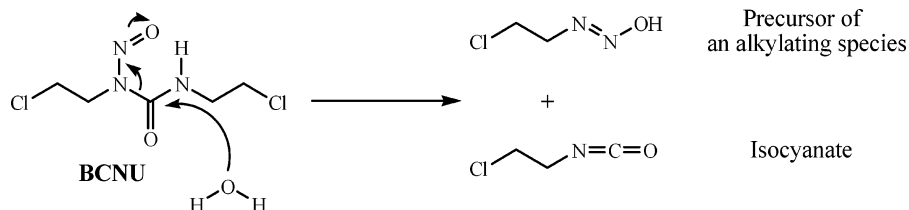


Figure 7. Growth inhibitory effects of amine **12** and nitrosourea **24** on the LNCaP/EGFR prostate cancer cell line. Cells were exposed to both drugs for 6 days, and growth inhibition measured using SRB assay. Each point represents at least two independent experiments run in triplicate.

that the antiproliferative potency of the stable nitrosourea **24** (IC_{50} (EGFR TK) = 294 nM) was approximately 3-fold greater than that of amine **12** (IC_{50} (EGFR TK) = 5 nM) that it is designed to release (see Figure 7). Also, it was more than 100-fold more potent than the clinical drug bis(2-chloroethyl)-*N*-nitrosourea (BCNU) (data not shown). The enhanced potency of **24** may be imputed to its ability to not only degrade to another inhibitor but also to release a DNA-alkylating species, as previously demonstrated for **22**.⁵

In summary, in the context of the combi-targeting principles, the combi-nitrosoureas (TZ-I), like other combi-molecules, were designed to degrade into an amine inhibitor (I) and the DNA-damaging metastable chloroethyl diazonium (TZ) species. These properties were previously demonstrated with FD137 (**22**), which was a weak EGFR TK inhibitor and presented an anomalously long half-life in serum-containing media ($t_{1/2} = 41$ h). On one hand, compounds **19–21** being primary nitrosoureas, although showing good EGFR TK inhibitory activities, have the potential to generate toxic isocyanates in a manner similar to that of the clinical drug BCNU²⁶ (Scheme 4). Their instability in serum-containing medium (see Table 1) will preclude their development as useful drugs. On the other hand,

Scheme 4. Decomposition of BCNU



free amines are reversible inhibitors deprived of alkylating functionalities. There thus remains the fact that the nitrosoureas methylated at N1 (**23** and **24**), that can be hydrolyzed to the amine inhibitor without the possibility of releasing toxic isocyanates and that show reasonable stability, are the most suitable for further development as useful drugs. The adverse effects of their high torsion angles are compensated by the 3'-halogens, which are less bulky than the methyl group of **22**, translating into 3–5-fold stronger inhibitory activity. Therefore, taking into account the EGFR TK affinity, the degradation half-life, the selectivity, and the antiproliferative potency, combi-molecule **23**, now referred to as **JDA58**, was considered to show the optimal profile and was chosen for further investigation. It has been recently selected by the National Cancer Institute (NCI) of the United States for further development under NSC no. 741282. A complete study characterizing its degradation in cells *in vitro* and *in vivo*, its mechanism of action, as well as its potency in a xenograft model in SCID mice will be reported shortly elsewhere.

3. Experimental Section

¹H NMR spectra and ¹³C NMR spectra were recorded on a Varian 400.14 or 300.06 spectrometer. Chemical shifts are expressed in parts per million (ppm) relative to the internal standard tetramethylsilane. Mass spectrometry was performed by the McGill University Mass Spectroscopy Center. Electrospray ionization (ESI) and atmospheric pressure chemical ionization (APCI) spectra were performed on a Finnigan LC QDUO spectrometer. High-resolution mass spectra (HMRS) were obtained from a ZAB-E4F analytical mass spectrometer. Data are reported as m/z (intensity relative to base peak = 100). The compounds were purified by flash chromatography using Caledon 50–200 μ m basic alumina or SiliCycle 40–63 μ m ultrapure silica gel. Melting points were determined in open capillary tubes on a Meltemp melting point apparatus and were uncorrected.

3.1. 4-Hydroxy-6-nitroquinazoline (2). 5-Nitroanthranilonitrile **1** (16.3 g, 100 mmol, 1.0 equiv) was added portionwise over 1 h to a mildly refluxing formic acid solution (200 mL) containing concentrated sulfuric acid (12 mL). After an additional 30 min, the solution was cooled to 0 °C and poured on crushed ice. The resulting precipitate was collected by filtration, washed with water, and dried to give 4-hydroxyquinazoline **2** (17.9 g, 90% yield). Mp 283–285 °C; ¹H NMR (400 MHz, DMSO-*d*₆) δ 12.72 (br, 1H, OH), 8.76 (d, 1H, $J = 2.8$ Hz, H-5), 8.50 (dd, 1H, $J = 8.8$ Hz, $J = 2.8$ Hz, H-7), 8.28 (s, 1H, H-2), 7.83 (d, 1H, $J = 8.8$ Hz, H-8); ¹³C NMR (100 MHz, DMSO-*d*₆) δ 159.7, 152.5, 148.6, 144.6, 128.7, 128.0, 122.4, 121.6.

3.2. *N*⁴-(3-Methylphenyl)-4,6-quinazolidineamine (7). A mixture of hydroxyquinazoline **2** (10.0 g, 52.4 mmol, 1.0 equiv) and PCl₅ (16.4 g, 78.5 mmol, 1.5 equiv) was melted and stirred for 2.5 h at 160 °C. The mixture was allowed to cool to room temperature, and the resulting solid was well washed with petroleum ether, filtered, and dried to give the 4-chloroquinazoline intermediate used directly in the next step.

4-Chloroquinazoline (4.8 g, 22.7 mmol, 1.0 equiv) was suspended in 2-propanol (25 mL), and 3-methylaniline (4.9 mL, 45.3 mmol, 2.0 equiv) was added. The resulting mixture was stirred at 60 °C overnight, the precipitate collected by hot filtration, washed with

2-propanol, water, diethyl ether, and dried under vacuum to give **4** (4.4 g, 70% yield). Mp 248–250 °C; ¹H NMR (400 MHz, DMSO-*d*₆) δ 10.35 (s, 1H, NH), 9.63 (s, 1H, H-5), 8.67 (s, 1H, H-2), 8.51 (dd, 1H, *J* = 9.2 Hz, *J* = 2.4 Hz, H-7), 7.88 (d, 1H, *J* = 9.2 Hz, H-8), 7.63 (d, 1H, *J* = 8.0 Hz, H-4'), 7.61 (s, 1H, H-2'), 7.28 (t, 1H, *J* = 7.8 Hz, H-5'), 7.69 (d, 1H, *J* = 7.8 Hz, H-6'), 2.34 (s, 3H, PhCH₃).

A suspension of **4** (5.5 g, 20.0 mmol, 1.0 equiv) and palladium (5% charcoal, 1.0 g, 9.4 mmol, 0.5 equiv) in methanol (100 mL) was hydrogenated at 2 bar for 1 h at room temperature. Filtration, evaporation, and chromatography on basic alumina with ethyl acetate gave **7** (2.8 g, 55% yield). Mp 245–248 °C; ¹H NMR (400 MHz, DMSO-*d*₆) δ 9.22 (br s, 1H, NH), 8.31 (s, 1H, H-2), 7.66 (s, 1H, H-5), 7.65 (d, 1H, *J* = 7.6 Hz, H-4'), 7.51 (d, 1H, *J* = 8.4 Hz, H-8), 7.35 (s, 1H, H-2'), 7.23–7.19 (m, 2H, H-5',7'), 6.86 (d, 1H, *J* = 7.6 Hz, H-6'), 5.54 (br s, 2H, NH₂), 2.31 (s, 3H, PhCH₃); ¹³C NMR (100 MHz, DMSO-*d*₆) δ 156.6, 150.5, 147.8, 143.2, 140.5, 138.0, 129.3, 128.8, 124.3, 124.2, 122.9, 119.6, 117.4, 101.8, 22.2.

3.3. N-(2-Cyano-4-nitrophenyl)-N,N-dimethylformamide (3). 5-Nitroanthranilonitrile **1** (48.9 g, 300 mmol, 1.0 equiv) was suspended in dimethylformamide dimethyl acetal (100 mL) and the mixture was refluxed for 1.5 h. The resulting mixture was cooled to room temperature and refrigerated overnight. The yellow precipitate that formed was filtered, washed with ethyl ether, and dried to give **3** (62.1 g, 95% yield). Mp 153–155 °C; ¹H NMR (400 MHz, DMSO-*d*₆) δ 8.43 (s, 1H, H-3), 8.24 (s, 1H, NCHN), 8.23 (d, 1H, *J* = 8.8 Hz, H-5), 7.34 (d, 1H, *J* = 8.8 Hz, H-6), 3.15 (s, 3H, NCH₃), 3.07 (s, 3H, NCH₃); ¹³C NMR (100 MHz, DMSO-*d*₆) δ 161.0, 157.3, 140.7, 130.1, 129.3, 119.0, 117.5, 106.6, 41.2, 35.3.

3.4. N⁴-(3-Chlorophenyl)-4,6-quinazolidinediamine (8). General Example of the Coupling Procedure. A mixture of **3** (21.8 g, 100 mmol, 1.0 equiv) and 3-chloroaniline (110 mmol, 1.1 equiv) was heated and stirred at reflux in acetic acid (100 mL) for 1 h. The yellow precipitate that formed was filtered hot, washed with hot acetic acid, diethyl ether, and dried to give the desired nitroquinazoline **5** (25.5 g, 85% yield). Mp 278–281 °C; ¹H NMR (400 MHz, DMSO-*d*₆) δ 10.40 (br s, 1H, NH), 9.57 (s, 1H, H-5), 8.71 (s, 1H, H-2), 8.49 (d, 1H, *J* = 9.2 Hz, H-7), 8.02 (s, 1H, H-2'), 7.88 (d, 1H, *J* = 9.2 Hz, H-8), 7.80 (d, 1H, *J* = 8.2, H-4'), 7.41 (t, 1H, *J* = 8.2, H-5'), 7.19 (d, 1H, *J* = 8.2, H-6'); ¹³C NMR (75 MHz, DMSO-*d*₆) δ 159.1, 158.0, 153.5, 145.2, 140.7, 133.4, 130.8, 130.2, 127.3, 124.6, 122.6, 121.5, 121.4, 115.1.

6-Nitroquinazoline **5** (8.0 g, 26.6 mmol, 1.0 equiv) and iron (10.0 g, 180 mmol, 7.0 equiv) were suspended in aqueous ethanol (700 mL, 70% v/v) containing acetic acid (24 mL, 360 mmol, 14 equiv) and heated at reflux until disappearance of starting material. The reaction mixture was cooled to room temperature and alkalized by addition of concentrated ammonia (150 mL). Insoluble material was removed by filtration through Celite, and the filtrate was evaporated under reduced pressure. The resulting solid was washed with 10% solution of K₂CO₃ and water until neutrality and dried in a desiccator over CaSO₄ to give amine **8** (5.8 g, 80% yield). Mp 235–237 °C; ¹H NMR (400 MHz, DMSO-*d*₆) δ 10.5 (br s, 1H, NH), 8.56 (s, 1H, H-2), 8.00 (br s, 1H, H-2'), 7.74 (dd, 1H, *J* = 8.0, *J* = 0.9 Hz, H-4'), 7.68 (d, 1H, *J* = 8.8 Hz, H-8), 7.56 (d, 1H, *J* = 1.6 Hz, H-5), 7.42–7.35 (m, 2H, H-7,5'), 7.21 (dt, 1H, *J* = 8.0, *J* = 0.9 Hz, H-6'), 5.50 (br s, 2H, NH₂); ¹³C NMR (100 MHz, DMSO-*d*₆) δ 157.8, 149.5, 147.7, 140.4, 135.3, 133.3, 130.8, 125.7, 125.0, 124.3, 123.4, 122.4, 116.6, 102.3.

3.5. N⁴-(3-Bromophenyl)-4,6-quinazolidinediamine (9). 6-Aminoquinazoline **9** was prepared as described for **8**. 6-Nitro-4-(3-bromophenyl)aminoquinazoline (**6**): 5.9 g, 86%; mp 267–270 °C; ¹H NMR (400 MHz, DMSO-*d*₆) δ 11.95 (br s, 1H, NH), 9.87 (d, 1H, *J* = 2.6 Hz, H-5), 9.0 (s, 1H, H-2), 8.73 (dd, 1H, *J* = 12.2 Hz, *J* = 2.6 Hz, H-7), 8.15 (d, 1H, *J* = 12.2 Hz, H-8), 8.04 (s, 1H, H-2'), 7.79 (d, 1H, *J* = 10.4 Hz, H-6'), 7.16–7.14 (m, 2H, H-4',5'); ¹³C NMR (100 MHz, DMSO-*d*₆) δ 159.2, 158.0, 153.2, 145.2, 140.7, 131.1, 130.0, 127.6, 127.5, 125.5, 122.0, 121.9, 121.5, 115.0. N⁴-(3-Bromophenyl)-4,6-quinazolidinediamine (**9**): 11.4 g, 83%; mp 204–206 °C; ¹H NMR (400 MHz, DMSO-*d*₆) δ 9.44 (s, 1H, NH),

8.37 (s, 1H, H-2), 8.20 (s, 1H, H-2'), 7.85 (d, 1H, *J* = 8.0 Hz, H-6'), 7.53 (d, 1H, *J* = 8.8 Hz, H-8), 7.32–7.20 (m, 4H, H-5, 7, 4', 5'), 5.66 (s, 2H, NH₂); ¹³C NMR (100 MHz, DMSO-*d*₆) δ 166.4, 156.2, 148.9, 143.7, 143.3, 131.5, 128.7, 124.9, 123.9, 121.8, 118.4, 114.9, 114.1, 99.5.

3.6. 4-[(3-Methylphenyl)amino]-6-(methylamino)quinazoline (10). General Example of the Reductive Methylation Procedure.

Amine **7** (1.0 g, 4.0 mmol, 1.0 equiv) was dissolved in anhydrous pyridine (20 mL), the solution was cooled to 0 °C in an ice bath, and 2-chloroethylchloroformate (0.4 mL, 4.4 mmol, 1.1 equiv) was added dropwise. Stirring continued at room temperature until disappearance of starting material as monitored by TLC (0.5–1 h). Pyridine was removed under reduced pressure, and the solid obtained was washed with 10% acetic acid solution and water until neutrality and dried giving carbamate, used directly in the next step. Ethyl carbamate (1.3 g, 4.0 mmol, 1.0 equiv) was dissolved in anhydrous THF (150 mL) and cooled in an ice bath. LiAlH₄ (0.6 g, 16.0 mmol, 4.0 equiv) was added by small doses, and mixture was heated at reflux until disappearance of starting material as monitored by TLC (1 h). The solution was cooled in an ice bath, and the excess of hydrate was destroyed with 30% KOH (4 equiv) solution. Insoluble materials were removed by filtration through Celite, and the filtrate was concentrated under reduced pressure. Chromatography on basic alumina eluting with ethyl acetate gave 6-methylamino-quinazoline **10** (0.37 g, 35% yield). Mp 115–117 °C; ¹H NMR (300 MHz, DMSO-*d*₆) δ 9.25 (s, 1H, NH), 8.29 (s, 1H, H-2), 7.65 (d, 1H, *J* = 7.8 Hz, H-8), 7.59 (s, 1H, H-5), 7.48 (d, 1H, *J* = 7.8 Hz, H-7), 7.26–7.18 (m, 2H, H-5',6'), 7.13 (d, 1H, *J* = 2.1 Hz, H-5'), 6.89 (d, 1H, *J* = 7.2 Hz, H-4'), 6.24 (q, 1H, *J* = 5.4 Hz, CH₃NH), 2.84 (d, 3H, *J* = 5.4 Hz, CH₃NH), 2.33 (s, 3H, PhCH₃); ¹³C NMR (75 MHz, DMSO-*d*₆) δ 156.6, 150.5, 149.0, 143.4, 140.3, 138.1, 129.1, 128.8, 124.5, 124.2, 123.4, 120.1, 117.3, 97.1, 31.0, 22.0.

3.7. 4-[(3-Chlorophenyl)amino]-6-(methylamino)quinazoline (11). 6-Methylaminoquinazoline **11** was prepared as described for **10**: 0.42 g, 37%; mp 133–134 °C; ¹H NMR (300 MHz, DMSO-*d*₆) δ 9.40 (s, 1H, NH), 8.37 (s, 1H, H-2), 8.06 (s, 1H, H-5), 7.84 (d, 1H, *J* = 8.0 Hz, H-6'), 7.53 (d, 1H, *J* = 7.8 Hz, H-8), 7.38 (t, 1H, *J* = 8.0 Hz, H-5'), 7.23 (d, 1H, *J* = 7.8 Hz, H-7), 7.12–7.10 (m, 2H, H-4',5'), 6.31 (q, 1H, *J* = 4.7 Hz, CH₃NH), 2.85 (d, 3H, *J* = 4.7 Hz, CH₃NH); ¹³C NMR (100 MHz, DMSO-*d*₆) δ 156.2, 150.1, 149.1, 143.6, 142.0, 133.3, 130.6, 129.2, 124.5, 123.1, 121.7, 120.7, 117.3, 96.8, 31.0.

3.8. 4-[(3-Bromophenyl)amino]-6-(methylamino)quinazoline (12). 6-Methylaminoquinazoline **12** was prepared as described for **10**: 0.43 g, 33%; mp 141–144 °C; ¹H NMR (400 MHz, DMSO-*d*₆) δ 9.39 (s, 1H, NH), 8.36 (s, 1H, H-2), 8.16 (t, 1H, *J* = 1.8 Hz, H-2'); 7.90 (md, 1H, *J* = 8.0 Hz, H-6'), 7.52 (d, 1H, *J* = 9.2 Hz, H-8), 7.32 (t, 1H, *J* = 8.0 Hz, H-5'), 7.25–7.18 (m, 2H, H-7,4'), 7.11 (d, 1H, *J* = 2.4 Hz, H-5), 6.33 (q, 1H, *J* = 5.2 Hz, CH₃NH), 2.84 (d, 3H, *J* = 5.2 Hz, CH₃NH); ¹³C NMR (75 MHz, DMSO-*d*₆) δ 156.2, 150.1, 149.1, 143.5, 142.2, 130.9, 129.2, 126.0, 124.5, 124.5, 121.8, 121.1, 117.3, 96.8, 31.0.

3.9. Standard Procedure for Preparation of 2-Chloroethyl Ureas (13–18). Amines **7–12** (1.0 mmol, 1.0 equiv) were dissolved in anhydrous THF (5 mL) and the solution was cooled to 0 °C in an ice bath. 2-Chloroethylisocyanate (130 μL, 1.5 mmol, 1.5 equiv) was added dropwise, and the reaction mixture was stirred until complete disappearance of the starting material. Thereafter, the solvent was evaporated, and the resulting solid was washed with 10% K₂CO₃, water, methylene chloride, and dried to give ureas **13–18** as off-white solids.

3.10. 1-(2-Chloroethyl)-3-[[4-(3-methylphenyl)amino]quinazolin-6-yl]urea (13): 0.34 g, 96%; mp 260–263 °C (dec); ¹H NMR (400 MHz, DMSO-*d*₆) δ 9.59 (s, 1H, Ar-NH-Ar); 8.90 (s, 1H, CONH-aryl), 8.43 (s, 1H, H-2), 8.34 (d, 1H, *J* = 2.3 Hz, H-5), 7.83 (dd, 1H, *J* = 8.8 Hz, *J* = 2.3 Hz, H-7), 7.67 (d, 1H, *J* = 8.8 Hz, H-8), 7.60 (s, 1H, H-2'), 7.59 (d, 1H, *J* = 7.6 Hz, H-6'), 7.23 (t, 1H, *J* = 7.6 Hz, H-5'), 6.89 (d, 1H, *J* = 7.6 Hz, H-4'), 6.64 (t, 1H, *J* = 6.0 Hz, ClCH₂CH₂NH), 3.69 (t, 2H, *J* = 6.0 Hz, ClCH₂-CH₂), 3.47 (q, 2H, *J* = 6.0 Hz, ClCH₂CH₂), 2.32 (s, 3H, PhCH₃);

^{13}C NMR (100 MHz, DMSO- d_6) δ 157.9, 155.7, 153.0, 145.8, 140.0, 138.8, 138.1, 128.9, 128.7, 126.9, 124.9, 123.5, 120.3, 116.3, 110.3, 45.2, 42.1, 22.1; MS (APCI $^+$) m/z 356.0 (MH $^+$ with ^{35}Cl), 358.0 (MH $^+$ with ^{37}Cl), 277.2 (M - ClEtNH - H, 10.7); HRMS (FAB $^+$) m/z calcd for C₁₆H₁₉N₅OCl, 356.127 813, found 356.127 670 (M + H) $^+$.

3.11. 1-(2-Chloroethyl)-3-[[4-(3-chlorophenyl)amino]quinazolin-6-yl]urea (14): 0.35 g, 94%; mp 254–256 °C (dec); ^1H NMR (400 MHz, DMSO- d_6) δ 9.98 (s, br, 1H, Ar-NH-Ar), 9.03 (s, 1H, CONH), 8.55 (s, 1H, H-2), 8.42 (d, 1H, $J = 1.8$ Hz, H-5), 8.02 (s, 1H, H-2'), 7.85 (dd, 1H, $J = 9.0$ Hz, $J = 1.8$ Hz, H-7), 7.77 (d, 1H, $J = 8.0$ Hz, H-4'), 7.72 (d, 1H, $J = 9.0$ Hz, H-8), 7.39 (t, 1H, $J = 8.0$ Hz, H-5'), 7.15 (d, 1H, $J = 8.0$ Hz, H-6'), 6.69 (t, 1H, $J = 5.9$ Hz, ClCH₂CH₂NH), 3.69 (t, 2H, $J = 5.9$ Hz, ClCH₂-CH₂), 3.23 (q, 2H, $J = 5.9$ Hz, ClCH₂CH₂); ^{13}C NMR (100 MHz, DMSO- d_6) δ 157.6, 155.6, 152.8, 146.1, 141.8, 139.0, 133.3, 130.7, 129.0, 127.0, 123.5, 121.9, 121.0, 111.4, 110.0, 45.2, 42.1; MS (ESI $^+$) m/z 376.1 (MH $^+$ with ^{35}Cl), 378.1 (MH $^+$ with ^{37}Cl), 342.1 (M - Cl + H, 27.0), 146.8 (M - ClEtNH - H, 46.0); HRMS (FAB $^+$) m/z calcd for C₁₇H₁₆N₅OCl₂, 376.073 191, found 376.073 120 (M + H) $^+$.

3.12. 1-(2-Chloroethyl)-3-[[4-(3-bromophenyl)amino]quinazolin-6-yl]urea (15): 0.39 g, 94%; mp 268–271 °C (dec); ^1H NMR (400 MHz, DMSO- d_6) δ 9.80 (s, 1H, Ar-NH-Ar), 8.96 (s, 1H, CONH), 8.51 (s, 1H, H-2), 8.39 (s, 1H, H-5), 8.16 (s, 1H, H-2'), 7.82–7.85 (m, 2H, H-6',7), 7.71 (d, 1H, $J = 9.2$ Hz, H-8), 7.32 (t, 1H, $J = 8.0$ Hz, H-5'), 7.26 (d, 1H, $J = 8.0$ Hz, H-4'), 6.65 (t, 1H, $J = 5.8$ Hz, ClCH₂CH₂NH), 3.69 (t, 2H, $J = 5.8$ Hz, ClCH₂CH₂), 3.47 (q, 2H, $J = 5.8$ Hz, ClCH₂CH₂); ^{13}C NMR (100 MHz, DMSO- d_6) δ 157.7, 155.6, 152.6, 145.3, 141.8, 139.1, 131.0, 128.5, 127.2, 126.6, 125.0, 121.8, 121.6, 116.3, 110.0, 45.2, 42.1; MS (APCI) m/z 420.0 (MH $^+$ with ^{79}Br , 64.8), 422.0 (MH $^+$ with ^{81}Br , 79.3), 341.0 (M - ClEtNH - H, with ^{79}Br , 10.0), 343.1 (M - ClEtNH - H, with ^{81}Br , 14.5); HRMS (FAB $^+$) m/z calcd for C₁₇H₁₆N₅OClBr, 420.022 674, found 420.022 780 (M + H) $^+$.

3.13. 3-(2-Chloroethyl)-1-methyl-1-[[4-(3-methylphenyl)amino]quinazolin-6-yl]urea (16): 0.35 g, 95%; mp 262–265 °C (dec); ^1H NMR (400 MHz, DMSO- d_6) δ 9.65 (s, 1H, Ar-NH-Ar), 8.56 (s, 1H, H-2), 8.45 (s, 1H, H-5), 7.75 (s, 2H, H-7,8), 7.66 (d, 1H, $J = 8.0$ Hz, H-6'), 7.64 (s, 1H, H-2'), 7.26 (t, 1H, $J = 8.0$ Hz, H-5'), 6.94 (d, 1H, $J = 8.0$ Hz, H-4'), 6.54 (t, 1H, $J = 5.6$ Hz, ClCH₂CH₂NH), 3.57 (t, 2H, $J = 6.8$ Hz, ClCH₂CH₂), 3.32 (q, 2H, $J = 6.8$ Hz, ClCH₂CH₂), 3.28 (s, 3H, NCH₃), 2.33 (s, 3H, PhCH₃); ^{13}C NMR (100 MHz, DMSO- d_6) δ 158.0, 157.9, 154.9, 148.2, 142.3, 139.6, 138.3, 133.3, 129.3, 129.0, 125.2, 123.4, 120.5, 120.2, 116.2, 44.2, 43.1, 38.0, 22.1; MS (ESI $^+$) m/z 370.2 (MH $^+$ with ^{35}Cl), 372.2 (MH $^+$ with ^{37}Cl), 265.2 (M - ClEtNHCO + H); HRMS (FAB $^+$) m/z calcd for C₁₉H₂₁N₅OCl, 370.143 463, found 370.143 450 (M + H) $^+$.

3.14. 3-(2-Chloroethyl)-1-methyl-1-[[4-(3-chlorophenyl)amino]quinazolin-6-yl]urea (17): 0.36 g, 93%; mp 232–235 °C (dec); ^1H NMR (400 MHz, DMSO- d_6) δ 9.79 (s, 1H, Ar-NH-Ar), 8.64 (s, 1H, H-2), 8.44 (s, 1H, H-5), 8.11 (s, 1H, H-2'), 7.84 (d, 1H, $J = 8.2$ Hz, H-4'), 7.79 (s, 2H, H-7,8), 7.41 (t, 1H, $J = 8.2$ Hz, H-5'), 7.16 (d, 1H, $J = 8.2$ Hz, H-6'), 6.57 (t, 1H, $J = 5.4$ Hz, ClCH₂CH₂NH), 3.58 (t, 2H, $J = 6.8$ Hz, ClCH₂CH₂), 3.23 (q, 2H, $J = 5.4$ Hz, ClCH₂CH₂), 3.28 (s, 3H, NCH₃); ^{13}C NMR (100 MHz, DMSO- d_6) δ 157.8, 157.3, 154.6, 148.3, 142.5, 141.4, 133.4, 130.8, 129.4, 123.8, 121.9, 120.9, 120.4, 116.1, 44.2, 43.1, 38.0; MS (ESI $^+$) m/z 390.2 (MH $^+$ with ^{35}Cl), 392.2 (MH $^+$ with ^{37}Cl), 356.2 (M - Cl + H with ^{35}Cl , 54.3), 358.2 (M - Cl + H with ^{37}Cl , 14.8), 285.4 (M - ClEtNHCO + H, 27.5); HRMS (FAB $^+$) m/z calcd for C₁₈H₁₈N₅OCl₂, 390.088 841, found 390.088 960 (M + H) $^+$.

3.15. 3-(2-Chloroethyl)-1-methyl-1-[[4-(3-bromophenyl)amino]quinazolin-6-yl]urea (18): 0.41 g, 94%; mp 253–255 °C (dec); ^1H NMR (400 MHz, DMSO- d_6) δ 9.78 (s, 1H, Ar-NH-Ar), 8.64 (s, 1H, H-2), 8.44 (s, 1H, H-5), 8.22 (t, 1H, $J = 2.0$ Hz, H-5), 7.91 (d, 1H, $J = 8.0$ Hz, H-6'), 7.79–7.78 (m, 2H, H-7,8), 7.35 (t, 1H, $J = 8.0$ Hz, H-5'), 7.29 (d, 1H, $J = 8.0$ Hz, H-4'), 6.57 (t, 1H, $J = 5.4$ Hz, ClCH₂CH₂NH), 3.58 (t, 2H, $J = 6.5$ Hz, ClCH₂CH₂),

3.32 (q, 2H, $J = 6.5$ Hz, ClCH₂CH₂), 3.28 (s, 3H, NCH₃); ^{13}C NMR (100 MHz, DMSO- d_6) δ 157.8, 157.3, 154.6, 148.3, 141.5, 133.5, 131.1, 129.4, 126.7, 124.7, 121.9, 121.2, 120.4, 116.1, 44.2, 43.1, 38.0; MS (APCI) m/z 434.1 (MH $^+$ with ^{79}Br , 74), 436.1 (MH $^+$ with ^{81}Br , 100), 329.3 (M - ClEtNHCO + H, with ^{79}Br), 331.1 (M - ClEtNHCO + H, with ^{81}Br); HRMS (FAB $^+$) m/z calcd for C₁₈H₁₈N₅OClBr, 434.038 324, found 434.038 210 (M + H) $^+$.

3.16. Standard Procedure for Preparation of Nitrosoureas (19–24). Ureas **13–18** (0.5 mmol, 1.0 equiv) were suspended in anhydrous acetonitrile (3 mL) containing acetic acid (43 μL , 0.75 mmol, 1.0 equiv), and the resulting solution was cooled to 0 °C in an ice bath. Nitrosonium tetrafluoroborate (88.5 mg, 0.75 mmol, 1.5 equiv) was added, and the reaction mixture was stirred at 0 °C until disappearance of starting material as monitored by TLC (3–4 h in the case of desmethylureas or overnight for N3-Me ureas). The reaction mixture was poured into 100 mL of ice-cooled water/ethyl acetate 1/1 solution, and the pH was adjusted to 5–6 by careful addition of 5% sodium bicarbonate solution. The water phase was extracted twice with ethyl acetate, and the organic extracts were washed with brine, dried over MgSO₄, and concentrated under reduced pressure without heating. Chromatography on silica gel eluting with a mixture of ethyl acetate/petroleum ether gave the expected nitrosoureas with moderate yield.

3.17. 1-(2-Chloroethyl)-1-nitroso-3-[[4-(3-methylphenyl)amino]quinazolin-6-yl]urea (19): 0.092 g, 48%; mp 135–137 °C (dec); ^1H NMR (400 MHz, DMSO- d_6) δ 11.01 (s, 1H, Ar-NH-Ar), 9.79 (s, 1H, CONH-aryl), 8.74 (s, 1H, H-5), 8.54 (s, 1H, H-2), 8.03 (d, 1H, $J = 8.8$ Hz, H-7), 7.80 (d, 1H, $J = 8.8$ Hz, H-8), 7.61 (s, br, 2H, H-2',6'), 7.26 (t, 1H, $J = 7.8$ Hz, H-5'), 6.94 (d, 1H, $J = 7.8$ Hz, H-4'), 4.22 (t, 2H, $J = 6.4$ Hz, ClCH₂CH₂), 3.73 (t, 2H, $J = 6.4$ Hz, ClCH₂CH₂), 2.33 (s, 3H, PhCH₃); ^{13}C NMR (100 MHz, DMSO- d_6) δ 158.2, 154.3, 152.0, 147.4, 139.7, 138.2, 135.9, 129.3, 128.9, 128.8, 125.1, 123.6, 120.4, 115.9, 115.5, 41.3, 22.1 (1C overlay with DMSO- d_6); MS (ESI $^+$) m/z 384.8 (MH $^+$ with ^{35}Cl , 15.7), 386.8 (MH $^+$ with ^{37}Cl , 4.2), 277.2 (M - ClEtNNO - H, 100.0); HRMS (FAB $^+$) m/z calcd for C₁₈H₁₈N₆O₂Cl, 385.117 977, found 385.118 090 (M + H) $^+$.

3.18. 1-(2-Chloroethyl)-1-nitroso-3-[[4-(3-chlorophenyl)amino]quinazolin-6-yl]urea (20): 0.103 g, 51%; mp 141–143 °C (dec); ^1H NMR (300 MHz, DMSO- d_6) δ 11.05 (s, 1H, Ar-NH-Ar), 9.97 (s, 1H, CONH), 8.76 (d, 1H, $J = 2.1$ Hz, H-5), 8.62 (s, 1H, H-2), 8.07 (dd, 1H, $J = 8.7$ Hz, $J = 2.1$ Hz, H-7), 8.05 (s, 1H, H-2'), 7.79–7.85 (m, 2H, H-4',8), 7.40 (t, 1H, $J = 7.9$ Hz, H-5'), 7.16 (d, 1H, $J = 7.9$ Hz, H-6'), 4.23 (t, 2H, $J = 6.2$ Hz, ClCH₂CH₂), 3.73 (t, 2H, $J = 6.2$ Hz, ClCH₂CH₂); ^{13}C NMR (75 MHz, DMSO- d_6) δ 158.0, 154.1, 152.1, 147.5, 141.5, 136.2, 133.4, 130.7, 129.5, 128.9, 123.8, 122.2, 121.2, 115.9, 115.2 (2C overlay with DMSO- d_6); MS (ESI $^+$) m/z 404.8 (MH $^+$ with ^{35}Cl), 406.8 (MH $^+$ with ^{37}Cl), 297.2 (M - ClEtNNO - H, with ^{35}Cl), 299.2 (M - ClEtNNO - H, with ^{37}Cl); HRMS (FAB $^+$) m/z calcd for C₁₇H₁₅N₆O₂Cl₂, 405.063 354, found 405.063 230 (M + H) $^+$.

3.19. 1-(2-Chloroethyl)-1-nitroso-3-[[4-(3-bromophenyl)amino]quinazolin-6-yl]urea (21): 0.108 g, 48%; mp 144–146 °C (dec); ^1H NMR (400 MHz, DMSO- d_6) δ 11.06 (s, 1H, Ar-NH-Ar), 9.97 (s, 1H, CONH), 8.75 (d, 1H, $J = 1.8$ Hz, H-5), 8.61 (s, 1H, H-2), 8.16 (s, 1H, H-2'), 8.06 (dd, 1H, $J = 9.2$ Hz, $J = 1.8$ Hz, H-7), 7.82–7.87 (m, 2H, H-6',8), 7.34 (t, 1H, $J = 7.8$ Hz, H-5'), 7.29 (d, 1H, $J = 7.8$ Hz, H-4'), 4.23 (t, 2H, $J = 6.4$ Hz, ClCH₂CH₂), 3.73 (t, 2H, $J = 6.4$ Hz, ClCH₂CH₂); ^{13}C NMR (100 MHz, DMSO- d_6) δ 158.1, 154.2, 152.1, 147.7, 141.7, 136.3, 131.1, 129.6, 129.0, 126.7, 125.0, 121.8, 121.6, 116.0, 115.2, 41.4 (1C overlay with DMSO- d_6); MS (ESI $^+$) m/z 450.9 (MH $^+$ with ^{79}Br), 452.9 (MH $^+$ with ^{81}Br), 341.1 (M - ClEtNNOCO - H, with ^{79}Br), 343.1 (M - ClEtNNOCO - H, with ^{81}Br); HRMS (FAB $^+$) m/z calcd for C₁₇H₁₅N₆O₂ClBr, 449.012 838, found 449.012 890 (M + H) $^+$.

3.20. 1-(2-Chloroethyl)-1-nitroso-3-methyl-3-[[4-(3-methylphenyl)amino]quinazolin-6-yl]urea (22): 0.100 g, 50%; mp 155–157 °C (dec); ^1H NMR (400 MHz, DMSO- d_6) δ 9.61 (s, 1H, Ar-NH-Ar), 8.54 (s, 1H, H-2), 8.53 (d, 1H, $J = 2.2$ Hz, H-5), 7.81 (dd, 1H, $J = 8.6$ Hz, $J = 2.2$ Hz, H-7), 7.73 (d, 1H, $J = 8.6$

Hz, H-8), 7.61–7.63 (m, 2H, H-2',6'), 7.26 (t, 1H, $J = 7.4$ Hz, H-5'), 6.95 (d, 1H, $J = 7.4$ Hz, H-4'), 4.06 (t, 2H, $J = 6.2$ Hz, ClCH_2CH_2), 3.70 (t, 2H, $J = 6.2$ Hz, ClCH_2CH_2), 3.59 (s, 3H, NCH_3), 2.33 (s, 3H, PhCH_3); ^{13}C NMR (100 MHz, $\text{DMSO}-d_6$) δ 158.1, 155.4, 148.4, 142.3, 139.4, 138.3, 132.5, 129.5, 129.0, 125.4, 123.5, 120.5, 120.2, 115.9, 42.9, 22.0 (2C overlay with $\text{DMSO}-d_6$); MS (ESI⁻) m/z 369.9 (M-1 with ^{35}Cl , 25.4), 398.9 (M-1 with ^{37}Cl , 6.5), 262.3 (M - ClEtNNO - H, with ^{35}Cl , 100.0), 263.2 (M - ClEtNNO - H, with ^{37}Cl , 29.6); HRMS (FAB+) m/z calcd for $\text{C}_{19}\text{H}_{20}\text{N}_6\text{O}_2\text{Cl}$, 399.133 627, found 399.135 550 (M + H)⁺.

3.21. 1-(2-Chloroethyl)-1-nitroso-3-methyl-3-[[4-(3-chlorophenyl)amino]quinazolin-6-yl]urea (23): 0.113 g, 54%; mp 140–142 °C (dec); ^1H NMR (400 MHz, CDCl_3) δ 9.76 (s, 1H, Ar-NH-Ar), 8.85 (s, 1H, H-2), 8.53 (d, 1H, $J = 1.8$ Hz, H-5), 8.07 (s, 1H, H-2'), 7.85 (dd, 1H, $J = 9.0$ Hz, $J = 1.8$ Hz, H-7), 7.75–7.81 (m, 2H, H-4',8), 7.41 (t, 1H, $J = 8.1$ Hz, H-5'), 7.17 (d, 1H, $J = 8.1$ Hz, H-6'), 4.07 (t, 2H, $J = 6.2$ Hz, ClCH_2CH_2), 3.71 (t, 2H, $J = 6.2$ Hz, ClCH_2CH_2), 3.60 (s, 3H, NCH_3); ^{13}C NMR (CDCl_3) δ 157.3, 154.9, 147.5, 142.9, 139.2, 134.8, 132.2, 130.3, 130.2, 125.0, 121.9, 119.8, 118.5, 115.3, 42.4, 41.9, 40.9; MS (ESI⁻) m/z 416.8 (M - 1 with ^{35}Cl , 30.2), 418.9 (M - 1 with ^{37}Cl , 17.3), 282.2 (M - ClEtNNOCO with ^{35}Cl , 100.0), 284.2 (M - ClEtNNOCO with ^{37}Cl , 31.7); HRMS (FAB+) m/z calcd for $\text{C}_{18}\text{H}_{17}\text{N}_6\text{O}_2\text{Cl}_2$, 419.079 004, found 419.079 000 (M + H)⁺.

3.22. 1-(2-Chloroethyl)-1-nitroso-3-methyl-3-[[4-(3-bromophenyl)amino]quinazolin-6-yl]urea (24): 0.114 g, 49%; mp 139–141 °C (dec); ^1H NMR (400 MHz, $\text{DMSO}-d_6$) δ 9.72 (s, 1H, Ar-NH-Ar), 8.64 (s, 1H, H-2), 8.54 (d, 1H, $J = 2.0$ Hz, H-5), 8.18 (t, 1H, $J = 2.0$ Hz, H-2'), 7.83–7.87 (m, 2H, H-6',7), 7.77 (d, 1H, $J = 8.8$ Hz, H-8), 7.35 (t, 1H, $J = 8.2$ Hz, H-5'), 7.30 (d, 1H, $J = 8.2$ Hz, H-4'), 4.07 (t, 2H, $J = 6.2$ Hz, ClCH_2CH_2), 3.70 (t, 2H, $J = 6.2$ Hz, ClCH_2CH_2), 3.60 (s, 3H, NCH_3); ^{13}C NMR (100 MHz, $\text{DMSO}-d_6$) δ 157.8, 155.2, 155.0, 148.5, 142.5, 141.2, 132.8, 131.1, 129.7, 126.9, 124.8, 121.9, 121.3, 120.4, 115.8, 42.9, 41.0; MS (APCI) m/z 462.8 (MH⁺ with ^{79}Br), 464.8 (MH⁺ with ^{81}Br), 432.2 (M - NO, with ^{79}Br), 434.2 (M - NO, with ^{81}Br), 328.2 (M - ClEtNNOCO, with ^{79}Br), 330.2 (M - ClEtNNOCO, with ^{81}Br); HRMS (FAB+) m/z calcd for $\text{C}_{18}\text{H}_{17}\text{N}_6\text{O}_2\text{ClBr}$, 463.028 488, found 463.028 640 (M + H)⁺.

3.23. Molecular Modeling. 3.23.1. PDB Structure Processing and Pocket Analysis 3.23.1.a. Alignment. The structures of the TK domain of EGFR, unbound and in complex with 4-anilinoquinazoline inhibitor, were downloaded from the PDB and aligned using the sequence and structural alignment application pro-Align in the 2004.03 version of the MOE software. The application default settings were used. The aligned structures had a high residue identity of 98.6% and a backbone aligned rmsd of 0.3849 Å.

3.23.1.b. Ligand Refinement in the Pocket. The ligand coordinates from the ligand-bound X-ray structure were used as a template to manually construct compounds **7–24** in the receptor pocket. A water molecule located near N1 in the quinazoline ring was also included in the calculations as it was crucial in order to retain more precise refined geometries. Each structure was minimized to a gradient of 0.01 kcal/Å mol in the presence of the fixed receptor atoms using the MMFF94x force field as implemented in MOE. The default force field settings were used. Each of the refined starting structures was then subjected to a systematic conformational search using the Csearch systematic conformational search routine in the MOE software. Each of the resulting conformations was refined by minimization in the fixed receptor pocket using the MMFF94x force field. The conformation with the lowest combined strain and receptor interaction energy was chosen as the representative bound pose for each compound and used for calculation of the van der Waals ligand/receptor interaction energy and the ligand strain energies. Dihedral angles between the quinazoline and ureido planes were read from Gaussian 98W software geometry-optimized structures. The Becke-style three-parameter density functional theory (B3LYP) method with the 3-21G basic set was used, and energy minima were confirmed by frequency calculations done with the same method and basic set.

3.23.2. Drug Treatment. Compounds were delivered dissolved in DMSO and subsequently diluted in sterile DMEM media containing 10% fetal bovine serum (FBS) (Life Technologies, Burlington, Canada) prior to addition to cell culture medium. The DMSO concentration never exceeded 0.2% (v/v).

3.23.3. Degradation. The study of the conversion of the nitrosoureas to their corresponding aminoquinazolines was performed by spectrofluorimetry as the latter amines were fluorescent (absorption 290 nm, emission 450 nm). Briefly, 125 mM of the nitrosoureas was added to RPMI-1640 with 10% FBS and incubated for 4 h at 37 °C in a microplate spectrofluorometer (SpectraMax Gemini fluorescence reader, Molecular Device, CA). The data are acquired and analyzed by SoftMaxPro (Molecular Device, CA).

Acknowledgment. We thank the U.S. Department of Defense (Award: DAMD17-03-0152) for financial support. We are also grateful to the Cancer Research Society Inc. (Montreal, Canada) for its continuous support of the development of the combi-targeting concept.

Supporting Information Available: NMR spectra, HRMS data, and HPLC chromatograms. This material is available free of charge via the Internet at <http://pubs.acs.org>.

References

- Brahimi, F.; Matheson, S. L.; Dudouit, F.; McNamee, J. P.; Tari, A. M.; Jean-Claude, B. J. Inhibition of epidermal growth factor receptor-mediated signaling by "combi-triazene" BJ2000, a new probe for combi-targeting postulates. *J. Pharmacol. Exp. Ther.* **2002**, *303*, 238–246.
- Matheson, S. L.; McNamee, J.; Jean-Claude, B. J. Design of a chimeric 3-methyl-1,2,3-triazene with mixed receptor tyrosine kinase and DNA damaging properties: a novel tumor targeting strategy. *J. Pharmacol. Exp. Ther.* **2001**, *296*, 832–40.
- Matheson, S. L.; Mzengeza, S.; Jean-Claude, B. J. Synthesis of a 1-[4-(*m*-tolyl)amino-6-quinazolyl]-3-[^{14}C]-methyl triazene: a radiolabeled probe for the combi-targeting concept. *J. Labelled Compds. Radiopharm.* **2003**, *46*, 729–735.
- Matheson, S. L.; McNamee, J.; Jean-Claude, B. J. Differential responses of EGFR/AGT-expressing cells to the "combi-triazene" SMA41. *Cancer Chemother. Pharmacol.* **2003**, *51*, 11–20.
- Qiu, Q.; Dudouit, F.; Banerjee, R.; McNamee, J.; Jean-Claude, B. J. Inhibition of cell signaling by the combi-nitrosourea FD137 in the androgen independent DU145 prostate cancer cell line. *Prostate* **2004**, *59*, 13–21.
- Qiu, Q.; Dudouit, F.; Matheson, S. L.; Brahimi, F.; Banerjee, R.; McNamee, J.; Jean-Claude, B. J. The combi-targeting concept: a novel 3,3-disubstituted nitrosourea with EGFR tyrosine kinase inhibitory properties. *Cancer Chemother. Pharmacol.* **2003**, *51*, 1–10.
- Meden, H.; Kuhn, W. Overexpression of the oncogene *c-erbB-2* (HER-2, neu) in ovarian cancer: a new prognostic factor. *Eur. J. Obstet. Gynecol. Reprod. Biol.* **1997**, *71*, 173–179.
- Modjtahedi, H.; Dean, C. The receptor for EGF and its ligands: expression, prognostic value and target for tumour therapy. *Int. J. Oncol.* **1998**, *4*, 277–296.
- Xinmei, C.; Yeung, T. K.; Wang, Z. Enhanced drug resistance in cells coexpressing *erb2* with EGF receptor or *erb3*. *Biochem. Biophys. Res. Commun.* **2000**, *277*, 757–763.
- Hsieh, S. S.; Malerczyk, C.; Aigner, A.; Czubayko, F. *erbB-2* expression is rate-limiting for epidermal growth factor-mediated stimulation of ovarian cancer cell proliferation. *J. Cancer* **2000**, *86*, 644–651.
- Roth, G. A.; Tai, J. J. A new synthesis of aryl substituted quinazolin-4(1*H*)-ones. *J. Heterocycl. Chem.* **1996**, *33*, 2051–2053.
- Morley, J. S.; Simson, J. C. E. The chemistry of simple heterocyclic systems. Part I. Reactions of 6- and 7-nitro-4-hydroxyquinazoline and their derivatives. *J. Chem. Soc.* **1948**, 360–366.
- Rewcastle, G. W.; Denny, W. A.; Bridges, A. J.; Hairong, Z.; Cody, D. R.; McMichael, A.; Fry, D. W. Tyrosine kinase inhibitor. Synthesis and structure-activity relationships for 4-[(phenylmethyl)amino]- and 4-(phenylamino)quinazolines as potent adenosine 5'-triphosphate binding site inhibitors of the tyrosine kinase domain of the epidermal growth factor receptor. *J. Med. Chem.* **1995**, *38*, 3482–3487.

- (14) Tsou, H.-R.; Mamuya, N.; Johnson, B. D.; Reich, M. F.; Gruber, B. C.; Ye, F.; Nilakantan, R.; Shen, R.; Discifani, C.; DeBlanc, R.; Davis, R.; Koehn, F. E.; Greenberger, L. M.; Wang, Y.-F.; Wissner, A. 6-Substituted-4-(3-bromophenylamino)quinazolines as putative irreversible inhibitors of the epidermal growth factor receptor (EGFR) and human epidermal growth factor receptor (HER-2) tyrosine kinases with enhanced antitumor activity. *J. Med. Chem.* **2001**, *44*, 2719–2734.
- (15) Bridges, A. J.; Zhou, H.; Cody, D. R.; Rewcastle, G. W.; McMichael, A.; Showalter, H. D. H.; Fry, D. W.; Kraker, A. J.; Denny, W. A. Tyrosine kinase inhibitors. 8. An unusually steep structure–activity relationship for analogues of 4-(3-bromoanilino)-6,7-dimethoxyquinazoline (PD 153035), a potent inhibitor of the epidermal growth factor receptor. *J. Med. Chem.* **1996**, *39*, 267–276.
- (16) Lown, J. W.; Chauhan, M. S. Synthesis of specifically ¹⁵N- and ¹³C-labeled antitumor (2-haloethyl)nitrosoureas. The study of their conformations in solution by nitrogen-15 and carbon-13 nuclear magnetic resonance and evidence for stereoelectronic control in their aqueous decomposition. *J. Org. Chem.* **1981**, *46*, 5309–5321.
- (17) Butler, R. N.; Lambe, T. M.; Tobin, J. C.; Scott, F. L. Stable heterocyclic primary nitroso-amines. *J. Chem. Soc., Perkin Trans. 1* **1973**, 1357–1361.
- (18) Smith, H. W.; Camerman, A. Molecular structure of 1-(2-chloroethyl)-3-(*trans*-4-methylcyclohexyl)-1-nitrosourea. *J. Med. Chem.* **1978**, *21*, 468–471.
- (19) Stamos, J.; Sliwkowski, M. X.; Eigenbrot, C. Structure of the epidermal growth factor receptor kinase domain alone and in complex with 4-anilinoquinazoline inhibitor. *J. Biol. Chem.* **2002**, *277*, 46265–46272.
- (20) Tanner, B.; Kreutz, W.; Meinert, R.; Knapstein, P. G.; Becker, R. Prognostic significance of c-erbB2 mRNA in ovarian carcinoma. *Gynecol. Oncol.* **1996**, *62*, 268–277.
- (21) Yen, L.; Zengrong, N.; You, X. L.; Richard, S.; Langton-Webster, B. C.; Aloui-Jamali, M. A. Regulation of cellular response to cisplatin-induced DNA damage and DNA repair in cells overexpressing p185neu is dependent on the ras signaling pathway. *Oncogene* **1999**, 1827–1835.
- (22) Hengstler, J. G.; Lange, J.; Kett, A.; Gornhofer, N.; Meinert, R.; Arand, M.; Knapstein, P. G.; Becker, R.; Oesch, F.; Tanner, B. Contribution of c-erbB-2 and topoisomerase II alpha to chemoresistance in ovarian cancer. *Cancer Res.* **1999**, *59*, 3206–3214.
- (23) Slamon, D. J.; Godolphin, W.; Jones, L. A.; et al. Studies of the HER-2/neu proto-oncogene in human breast and ovarian cancer. *Science* **1989**, *244*, 707–712.
- (24) Banerjee, R.; Rachid, Z.; McNamee, J.; Jean-Claude, B. J. Synthesis of a prodrug designed to release multiple inhibitors of the epidermal growth factor receptor tyrosine kinase and an alkylating agent: a novel tumor targeting concept. *J. Med. Chem.* **2003**, *46*, 5546–5551.
- (25) Rachid, Z.; Brahim, F.; Domarkas, J.; Jean-Claude, B. J. Synthesis of half-mustard combi-molecules with fluorescence properties: correlation with EGFR status. *Bioorg. Med. Chem. Lett.* **2005**, *15*, 1135–1138.
- (26) Colvin, M.; Brundrett, R. Chemical decomposition of chloroethyl-nitrosoureas. *Nitrosoureas Current Status and New Developments*; Prestayako, A. W., et al., Eds.; Academic Press: 1981, 43–49.

JM0600390